

1 ***In silico* cancer immunotherapy trials uncover the consequences of therapy-specific response**  
2 **patterns for clinical trial design and outcome**

3 Jeroen H.A. Creemers<sup>1,2</sup>, Kit C.B. Roes<sup>3</sup>, Niven Mehra<sup>4</sup>, Carl G. Figdor<sup>1,2</sup>, I. Jolanda M. de Vries<sup>1</sup>,  
4 Johannes Textor<sup>1,5\*</sup>

- 5  
6 1) Department of Tumor Immunology, Radboud Institute for Molecular Life Sciences,  
7 Radboudumc, Nijmegen, The Netherlands  
8 2) Oncode Institute, Nijmegen, The Netherlands  
9 3) Department of Health Evidence, Section Biostatistics, Radboudumc, Nijmegen, The  
10 Netherlands  
11 4) Department of Medical Oncology, Radboudumc, Nijmegen, The Netherlands  
12 5) Data Science Department, Institute for Computing and Information Sciences, Radboud  
13 University, Nijmegen, The Netherlands

14  
15 \* Corresponding author:

16 Dr. J. Textor

17 Department of Tumor Immunology

18 Radboud Institute for Molecular Life Sciences, Radboudumc

19 Geert Grooteplein 26

20 6500 HB Nijmegen (P.O. Box 9101), The Netherlands

21 E-mail: [johannes.textor@radboudumc.nl](mailto:johannes.textor@radboudumc.nl)

22 Phone: 0031-24 361 76 00  
23  
24

25 **ABSTRACT**

26 **Background**

27 Late-stage cancer immunotherapy trials strive to demonstrate the clinical efficacy of novel  
28 immunotherapies, which is leading to exceptional responses and long-term survival in subsets of  
29 patients. To establish the clinical efficacy of an immunotherapy, it is critical to adjust the trial's design  
30 to the expected immunotherapy-specific response patterns.

31 **Methods**

32 *In silico* cancer immunotherapy trials are virtual clinical trials that simulate the kinetics and outcome  
33 of immunotherapy depending on the type and treatment schedule. We used an ordinary differential  
34 equation model to simulate (1) cellular interactions within the tumor microenvironment, (2) translates  
35 these into disease courses in patients, and (3) assemble populations of virtual patients to simulate *in*  
36 *silico* late-stage immunotherapy, chemotherapy, or combination trials. We predict trial outcomes and  
37 investigate how therapy-specific response patterns affect the probability of their success.

38 **Results**

39 *In silico* cancer immunotherapy trials reveal that immunotherapy-derived survival kinetics – such as  
40 delayed curve separation and plateauing curve of the treatment arm – arise naturally due to biological  
41 interactions in the tumor microenvironment. *In silico* clinical trials are capable of translating these  
42 biological interactions into survival kinetics. Considering four aspects of clinical trial design – sample  
43 size calculations, endpoint and randomization rate selection, and interim analysis planning – we  
44 illustrate that failing to consider such distinctive response patterns can significantly reduce the power  
45 of novel immunotherapy trials.

46 **Conclusion**

47 *In silico* trials have three significant implications for immuno-oncology. First, they provide an  
48 economical approach to verify the robustness of biological assumptions underlying an immunotherapy  
49 trial and help to scrutinize its design. Second, the biological basis of these trials facilitates and  
50 encourages communication between biomedical researchers, doctors, and trialists. Third, its  
51 application as an educational tool can illustrate design principles to scientists in training, contributing  
52 to improved designs and higher success rates of future immunotherapy trials.

NOTE: This preprint reports new research that has not been certified by peer review and should not be used to guide clinical practice.

## 53 INTRODUCTION

54 Immunotherapy is revolutionizing the treatment landscape for patients with advanced  
55 cancers. While the number of immuno-oncology drugs under investigation is rising rapidly – around  
56 4700 agents are currently in the development pipeline - the need to further improve patient outcomes  
57 remains high<sup>1</sup>. Well-designed immunotherapy trials are crucial to establish advances in clinical  
58 outcomes robustly. Unfortunately, the odds for cancer treatments to successfully pass the  
59 development pipeline are unfavorable, and only a minority of the treatments (5-10%) will ultimately  
60 obtain market approval<sup>2, 3, 4</sup>. Even for cancer therapies that reach late-stage development, approval  
61 rates remain modest at around 27%<sup>5</sup>. The primary reason in most of these trials (i.e., 63.7%) is failure  
62 to demonstrate efficacy<sup>5</sup>, which can be partly attributed to suboptimal trial design choices based on  
63 overly optimistic assumptions of the treatment effect. Such assumptions may be used to erroneously  
64 justify low numbers of patients or inappropriate endpoints and lower the power of these trials<sup>5, 6</sup>.

65 Undoubtedly, design choices in immunotherapy trials are complex, and conventional design  
66 methods are not naturally well attuned to the unique characteristics of immunotherapies<sup>7</sup>. Their broad  
67 spectrum – ranging from immunomodulators to cell therapies, cancer vaccines, oncolytic viruses, and  
68 CD3-targeted bispecific antibodies – illustrates the variety in molecular mechanisms, leading to novel  
69 toxicity profiles, response patterns, and survival kinetics<sup>8, 9, 10</sup>. These observations render a ‘one-  
70 design-fits-all’ approach futile and stress the need for immunotherapy- or even combination-therapy-  
71 tailored designs.

72 Immunotherapies are known to induce a delayed clinical effect and long-term overall survival  
73 (OS) in only a subset of patients<sup>11</sup>. The survival curve reflects these phenomena by a delayed curve  
74 separation and a plateau of the treatment arm at later stages of the trial, respectively<sup>12</sup>. Many  
75 immunotherapies, thereby, violate a fundamental premise that underlies the design of many trials: the  
76 proportional hazard assumption (PHA) – essentially stating that the treatment effect should remain  
77 constant over time<sup>13</sup>. As a result, immunotherapy trials based on this principle can have an  
78 overestimated power<sup>12, 13</sup> and require a longer follow-up to demonstrate efficacy than initially  
79 planned<sup>12</sup>, increasing the likelihood of a negative trial.

80 These issues led to the development of innovative methods such as novel radiological criteria  
81 to quantify tumor responses<sup>9, 14, 15</sup>, (surrogate) endpoints to capture unique survival kinetics<sup>10, 16, 17, 18,</sup>  
82 <sup>19</sup>, biomarkers to enrich for potentially responding patients for treatment<sup>20, 21, 22, 23</sup>, and statistical  
83 methods to retain a trial’s power in the presence of non-conventional survival kinetics<sup>24, 25, 26</sup>. Despite  
84 the plethora of available methods, it still remains complicated to predict trial outcomes *in advance* and  
85 adjust the methodology accordingly. The stakes are high: accurate predictions could augment the  
86 likelihood of a positive trial, whereas a misjudgment could result in a negative trial, potentially  
87 compromising patient benefit, vast amounts of work, and (public) research funds.

88 In this study, we use late-stage *in silico* cancer immunotherapy trials to investigate how design  
89 decisions affect the trial outcome in the context of cancer immunotherapy, possibly combined with  
90 chemotherapy. The mechanism-based nature of these trials allows researchers to translate cellular  
91 processes in the tumor microenvironment and interventions thereon into immunotherapy-specific  
92 response patterns, survival kinetics, and outcomes of novel immunotherapy trials. An *in silico*  
93 immunotherapy trial is based on clear-cut biological assumptions and provides an intuitive means to  
94 predict risk profiles and treatment efficacy. Moreover, it equips researchers with a tool to verify trial  
95 designs and analysis strategies of upcoming trials before the trials' execution. First, we show that our  
96 simulations replicate late-stage immunotherapy or combination trials realistically and capture their  
97 typical survival kinetics. Then, we demonstrate various applications of these trial simulations, including  
98 the ability to predict the trial outcomes and calculate sample sizes for specific treatment and control  
99 groups. Finally, we illustrate the consequences of (not) considering immunotherapy-specific response  
100 patterns in settings selected for educational purposes, such as selecting survival endpoints and  
101 randomization ratios of upcoming trials and planning interim analyses.

102

## 103 **METHODS**

### 104 **Mechanism-based model of the tumor microenvironment**

105 We extended our previously published ordinary differential equation (ODE) model that describes  
106 cancer development in the tumor microenvironment and the subsequently induced anti-tumor  
107 response in patients<sup>27</sup>. Briefly, the model describes cancer onset and progression, starting with the  
108 malignant degeneration of a single cell into a tumor cell. This tumor cell divides, leading to a  
109 proliferating mass ( $\rho$ : growth rate) of tumor cells (T; equation 1; Figure 1A). An anti-tumor immune  
110 response is induced within the tumor microenvironment, leading to the killing of tumor cells (at killing  
111 rate  $\xi$ ; equation 1). The killing of tumor cells is implemented using a quasi-steady state approximation  
112 proposed by Borghans *et al.*<sup>28,29</sup>. For details on the implementation, we refer to our previous work<sup>27</sup>.  
113 The immune cells within the tumor microenvironment originate from tumor-draining lymph nodes,  
114 where naive cytotoxic T cells (N) turn into activated T cells (S) at priming rate  $\alpha$ . Since a larger tumor  
115 mass is generally more immunogenic, the priming rate is scaled by the tumor size ( $\frac{T}{10+T}$ ; equations 3  
116 and 4). Primed T cells proliferate in the lymph nodes at rate  $p_s$  and migrate into the tumor  
117 microenvironment at rate  $m_s$  (equation 2). The natural life span of T cells in the tumor  
118 microenvironment is modeled by incorporating a natural death rate  $\delta$  of T cells. The system of ODEs is  
119 presented below:

120

$$\left\{ \begin{array}{l} \frac{dT}{dt} = \rho T^{\frac{4}{5}} - \frac{\xi I T}{1 + \frac{I}{h_I} + \frac{T}{h_T}} \quad (Eq. 1) \\ \frac{dI}{dt} = m_s S - \delta I \quad (Eq. 2) \\ \frac{dS}{dt} = \alpha \left( \frac{T}{10^7 + T} \right) N + p_s S - m_s S \quad (Eq. 3) \\ \frac{dN}{dt} = -\alpha \left( \frac{T}{10^7 + T} \right) N \quad (Eq. 4) \end{array} \right.$$

121

122

Table 1: Overview of model parameters

Interpatient variability	Symbol	Parameter	Default value or range	Description
Variable	$\rho$	Tumor growth rate (cells/day)	1.76 - 150	Growth rate of tumor cells
	$\Delta\rho$	Growth rate decline	-0.6 - 0	Rate at which tumor cell proliferation declines over time
	$\rho_\delta$	Growth rate decline decay	-2 - 0	Rate at which the tumor growth rate decline decreases.
Universal	$\xi$	Relative T cell killing rate (cells/day)	0.001	Killing rate of cytotoxic T cells
	$\alpha$	T cell priming rate (cells/day)	0.0025	Rate at which antigen-specific T cells are activated
	$\delta$	T cell death rate (cells/day)	0.019	Death rate of T cells
	$h$	Michaelis constant (cells)	571	Ratio between tumor-immune cell complex formation and dissociation
	$p_s$	Production rate (cells/day)	1	Production rate of T cells from lymph nodes
	$m_s$	Migration rate (cells/day)	1	T cell migration rate from lymph node to tumor microenvironment

123

124

125

126

Since a constant time-independent tumor growth rate would unlikely be observed in a clinical setting, we have added two additional parameters to the model that influence the growth rate of tumors in a time-dependent manner, which are:

127

128

129

130

- The tumor growth rate decline ( $\Delta\rho$ ): a parameter that describes to which extent the proliferation rate of tumor cells gradually declines over time.
- The decay rate of the tumor growth rate decline ( $\rho_\delta$ ; hereafter referred to as ‘decline decay rate’): a parameter that indicates at which pace the tumor growth rate decline decreases.

131

132

133

134

135

136

The model parameters and their values are listed in Table 1; their rationale is described previously<sup>27</sup>. Moreover, the values of the tumor growth rate decline and its decay rate were set to augment the interpatient variability in tumor development and allow for more extensive disease trajectories. At baseline, only one tumor cell and a pool of  $10^6$  naive T cells are presumed to be present, while activated T cells are absent, yielding the following initial conditions for the simulations:  $T(0) = 1$ ,  $I(0) = 0$ ,  $S(0) = 0$ , and  $N(0) = 10^6$ .

137

### 138 **Simulating untreated disease, chemotherapy, and immunotherapy in individual patients**

139 Using this ODE model, we simulated cancer development and disease trajectories in patients. We  
140 varied the tumor properties (i.e., the tumor growth rate, the growth rate decline, and the decline decay  
141 rate) between patients extensively to guarantee interpatient variation in disease courses. Unless  
142 otherwise specified, the remaining model parameters are set to the same values for all patients (Table  
143 1).

144 Each patient is simulated from cancer onset (i.e., malignant transformation of the first cell) for  
145 up to more than two years (i.e., 800 days). A simulated time step corresponds to one day. The diagnosis  
146 threshold of a tumor mass was set to  $65 * 10^8$  cells, corresponding to the size at which common  
147 malignancies are diagnosed. The lethal tumor burden is set to  $10^{12}$  tumor cells (a tumor volume of  
148 approximately  $10.6 \text{ dm}^3$ ).

149 Disease trajectories of patients with cancer can be steered with therapy. Given their prominent  
150 roles in the oncological treatment landscape, we included immune checkpoint inhibitors (ICI) and  
151 chemotherapy in the model. Both treatments function through their primary modes of action. ICI are  
152 implemented as follows: once a cancer reaches a diagnosis threshold, immune checkpoint inhibitors  
153 increase the killing rate of cytotoxic T cells (multiplication factor: 0-7), enabling them to eradicate  
154 tumor cells. The duration and potency of the ICI treatment eventually determines patient outcome.

155 In patients treated with chemotherapy, the immune system is still present; however, it is not  
156 boosted (as is the case during ICI treatment), hence the T cells are not potent enough to curb the tumor  
157 growth. Once a patient is diagnosed with cancer, chemotherapy can reduce the tumor growth rate  
158 with its cytotoxic capacity (multiplication factor: 0-1). Again, the duration and potency determine  
159 patient outcome. By default, the treatment duration for ICI and chemotherapy are two years and six  
160 months, respectively.

161

### 162 **Simulating untreated cohorts in an *in silico* trial: model fitting**

163 To expand our modeling approach from a single patient into a trial cohort, we simulated multiple  
164 patients with individualized disease courses based on unique tumor properties. As an illustrative  
165 example, we took a publicly available dataset of patients with advanced lung cancer from the North  
166 Central Cancer Treatment Group (NCCTG) and regarded the survival times of these patients as if they  
167 were untreated<sup>30</sup>. We fitted our model to the NCCTG dataset to show that our trial model can  
168 reproduce authentic survival kinetics as observed in clinical trials. Specifically, we searched for  
169 parameter combinations reflecting realistic survival times for each patient in our model. Since a single-  
170 parameter fitting approach could not generate a sufficiently wide range of survival times, we used a

171 multidimensional fitting approach. An overview of the fitting approach is depicted in Supplementary  
172 Figure 1.

173 Specifically, we fitted the tumor growth rate ( $\rho$ ), the decline in tumor growth rate over time  
174 ( $\Delta\rho$ ), and the decline's decay rate ( $\rho_\delta$ ) of patients to OS. The fitting approach comprised two processes:  
175 1) sampling non-censored survival values and 2) translating these survival values to model parameters.  
176 We fitted a (parametric) Weibull distribution to the NCCTG lung cancer dataset (shape  $\kappa$ : 1.32, scale  $\lambda$ :  
177 417.76; Supplementary figure 1A). The choice for a Weibull distribution is based on the Akaike  
178 information criterion and the fact that a Weibull model is a survival model from which the parameters  
179 (i.e., scale and shape) contain a mechanistic meaning and can, therefore, be interpreted. From the  
180 Weibull distribution, non-censored survival values were sampled (Supplementary figure 1B). To  
181 translate the survival times into model parameters, we generated a 3D grid containing survival times  
182 for ranges of parameters ( $\rho$ : 1.76 – 150,  $\Delta$ : -0.6 - 0,  $\rho_\delta$ : -2 - 0; Supplementary figure 1C). From this grid,  
183 combinations of these three parameters that led to a similar OS (i.e., the isosurfaces) were extracted  
184 with a marching cubes algorithm (Supplementary figure 1D). The isosurfaces corresponding to the non-  
185 censored survival times from the Weibull distribution were selected, and parameter combinations  
186 were sampled from these isosurfaces randomly (Supplementary figure 1E). To illustrate that these  
187 parameter combinations led to realistic survival kinetics as seen in clinical trials, we compared the  
188 original NCCTG lung cancer dataset with our simulation result (Supplementary figure 1F; Figure 1).

189

### 190 **Simulating late-stage immunotherapy trials**

191 Late-stage (i.e., phase III) clinical trials traditionally contain two arms: a control arm and a treatment  
192 arm. The control arm can be a placebo (i.e., untreated) or a standard of care therapy. To construct  
193 phase III *in silico* immunotherapy trials, we extended the simulations with treatment cohorts (mono-  
194 chemotherapy, mono-immunotherapy, chemoimmunotherapy, or induction chemotherapy followed  
195 by immunotherapy). These cohorts facilitate the comparison between various treatment regimens. A  
196 treatment cohort uses the same baseline parameter distribution as a control cohort. It differs in one  
197 critical aspect, though: once patients in the treatment arm reach a tumor burden that corresponds to  
198 the diagnosis threshold, patients can be treated with chemotherapy, ICI, or combination therapy, as  
199 described above. The distribution of survival parameters is, unless otherwise specified, derived from  
200 the most mature, digitized data from the CA184-024 trial, as shown below<sup>31</sup>. At inclusion into the trial,  
201 patients are randomly assigned to a study arm (randomization).

202 The primary endpoint of the trials is the 2-year OS. Given the absence of accrual times in *in*  
203 *silico* trials, the trial duration equals two years, which provides each patient in the trial with 24 months

204 follow-up at the time of analysis. If the OS endpoint is not reached for a patient, the patient is  
205 considered censored for the endpoint and regarded as such in subsequent analyses.

206

### 207 **Power simulations**

208 To illustrate how the analysis method can affect the outcome of immunotherapy trials, we use several  
209 simulation approaches to calculate the power of trials. Power simulations were performed as follows:  
210 per data point, 1000 clinical trials are simulated. The survival data from each trial is analyzed with a  
211 log-rank test (dependent on the proportional hazard assumption) or proportions test (Pearson's chi-  
212 squared test; independent on the proportional hazard assumption), and we count the number of  
213 positive trials (defined as  $p < 0.05$ ). The percentage of positive trials indicates the power of the trial.

214

### 215 **Data digitization & reconstruction**

216 For some survival curves, the raw data was not available. Therefore, we extracted data points from  
217 the Kaplan-Meier curves with WebPlotDigitizer (<https://apps.automeris.io/wpd/>), and individual  
218 patient data was reconstructed with the IPDfromKM package in R.

219

### 220 **Analyses**

221 Analyses and visualizations were performed in R. The complete list of R packages used throughout this  
222 manuscript is provided in Supplementary Table 1. The code is accessible via  
223 <https://github.com/jeroencreemers/in-silico-clinical-trials>.

224

## 225 RESULTS

### 226 Generating trial populations based on tumor-immune dynamics

227 We used *in silico* cancer immunotherapy trials – a mechanism-based simulation platform of cancer-  
228 immune dynamics – to investigate the consequences of immunotherapy-specific response patterns on  
229 trial design principles<sup>27</sup>. Patients within these trials are simulated with an ODE model, which describes  
230 cancer development in a patient by modeling the interaction between tumor cells and the immune  
231 system<sup>27</sup>. In short, the model describes the following tumor-immune dynamics in the tumor  
232 microenvironment: immunogenic tumor growth leading to priming and clonal expansion of T cells in  
233 the lymph nodes, migration of effector T cells from lymph node to the tumor microenvironment, and  
234 formation of tumor-immune complexes to enable tumor cell killing (see Methods; Figure 1A). The  
235 model allows the treatment of patients with ICI and chemotherapy. ICI increase the killing rate of T  
236 cells and have a direct effect on the tumor-immune dynamics. Chemotherapy has a cytotoxic effect on  
237 the tumor, slowing down its growth rate. A detailed description of the model, including the rationale  
238 for parameter selection, has been published previously<sup>27</sup>.

239 The *in silico* clinical trials describe cancer outcomes on three levels: (1) a cellular level, (2) a  
240 patient level, and (3) a trial population level. Cellular interactions in the tumor microenvironment are  
241 translated into clinical trial outcomes as follows: firstly, the ODE model is implemented, and model  
242 parameters are selected using a fitting approach (Figure 1B; see Methods). Next, individualized disease  
243 trajectories – either treated or untreated – of cancer patients are generated (Figure 1C). Eventually,  
244 patients are randomized into two cohorts to resemble conventional phase III trials: a control group  
245 (either placebo or chemotherapy) and a treatment group (immunotherapy, chemoimmunotherapy, or  
246 induction chemotherapy followed by immunotherapy; Figure 1D). Since the cellular dynamics (e.g.,  
247 tumor burden over time or the efficacy of T cell killing) and survival outcomes of these patients are  
248 known and can be modified, *in silico* clinical trials are suited to answer questions like: “Assuming that  
249 a novel treatment X increases T cell killing by 5%, how does this translate to a survival benefit in  
250 patients? Moreover, how many patients are needed to establish this benefit in a clinical trial? When  
251 should one analyze the results?” (Figure 1E).

252



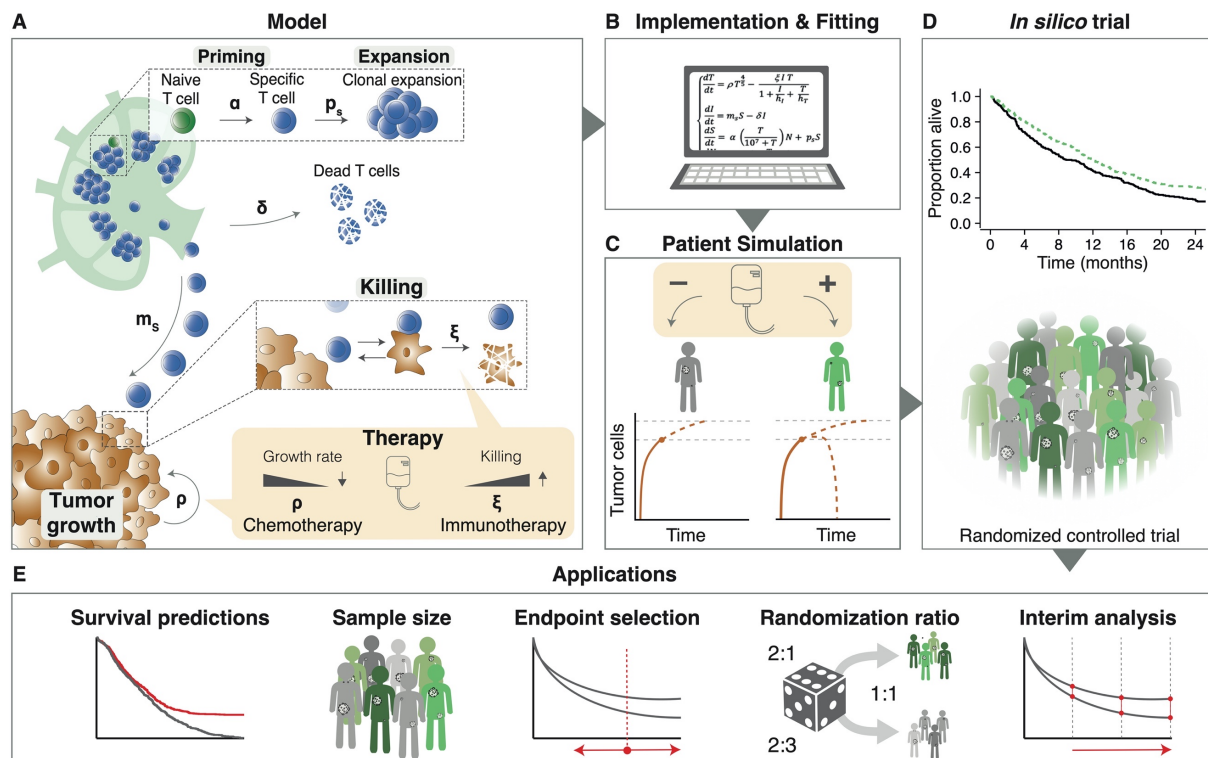


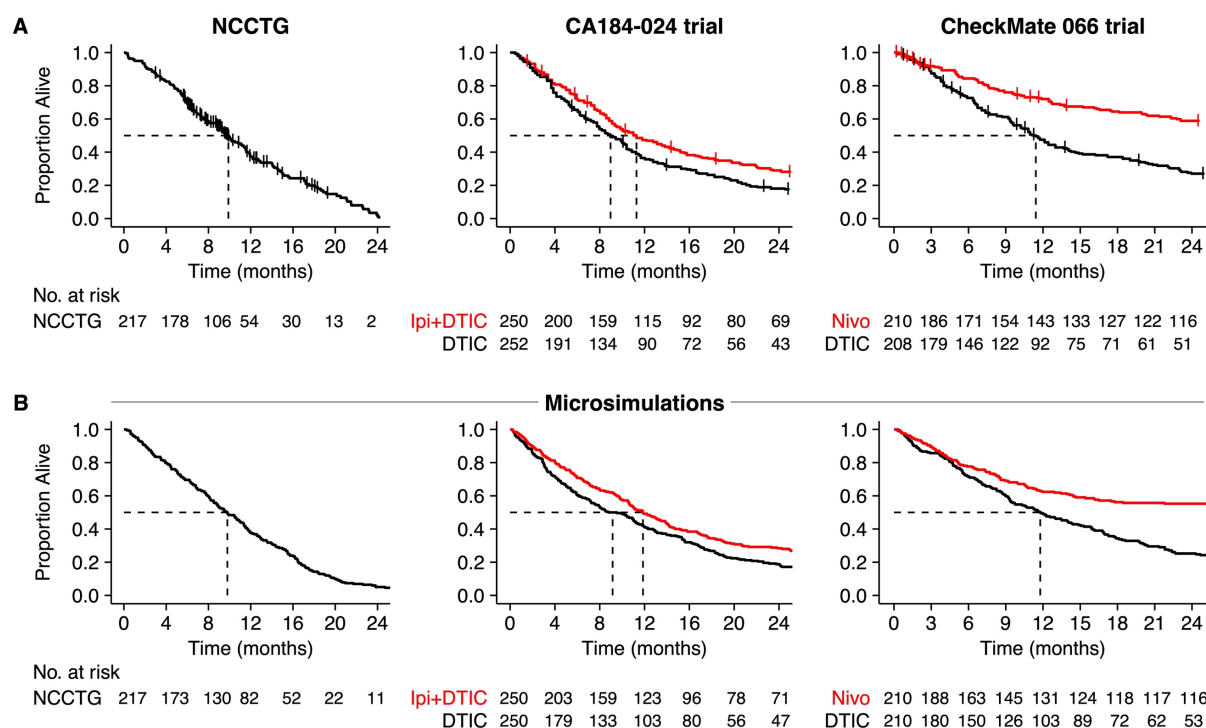
**Figure 1: *In silico* late-stage immunotherapy trials and their applications.**

(A) Cellular interactions between a tumor and the immune system are captured in an ODE model. This model describes immunogenic tumor growth leading to a T cell response originating from lymph nodes. Disease courses in patients could be steered by immunotherapy, chemotherapy, or a combination of both. Parameters:  $\alpha$  = naive T cell priming rate,  $\delta$  = effector T cell death rate,  $\xi$  = effector T cell killing rate,  $\rho$  = tumor growth rate,  $p_s$  = effector T cell proliferation rate, and  $m_s$  = effector T cell migration rate. (B) After implementation, we used clinical trial-derived survival data to fit the model parameters (see Suppl. Figure 1). (C) Patients received either no treatment (placebo), chemotherapy, immunotherapy, or both. Disease trajectories based on tumor-immune dynamics were simulated for each patient, resulting in individual survival outcomes. (D) Subsequently, cohorts of patients were constructed based on the fitted parameters to simulate actual immunotherapy trials. (E) Applications of these trials include predicting survival outcomes of trials, estimating appropriate sample sizes, selecting endpoints and randomization ratios, and investigating the timing of interim analyses.

### ***In silico* late-stage immunotherapy trials yield realistic survival outcomes**

To illustrate that this *in silico* clinical trial approach can generate realistic survival kinetics as observed in late-stage immunotherapy trials, we fitted the simulation to three different datasets: (1) the NCCTG lung cancer survival dataset<sup>30</sup>; (2) the CA184-024 trial [ipilimumab + dacarbazine vs. dacarbazine in previously untreated metastatic melanoma<sup>31</sup>]; and (3) the CheckMate 066 trial [nivolumab + placebo vs. dacarbazine + placebo in treatment-naïve metastatic melanoma patients without BRAF mutation<sup>32</sup>]. The choice for these trials is based on the size of the trials and the maturity of the data. The follow-up of the CA184-024 trial and the CheckMate 066 trial were five and three years, respectively. As the last two datasets were not publicly available, we extracted the data using image digitization (see Methods). As a reference for the *in silico* trials, we visualized the Kaplan-Meier estimators of these datasets (Figure 2A). Both trials were digitized correctly, as reflected by the nearly identical risk tables compared to the original manuscripts<sup>31, 32</sup>. Next, we fitted our trial simulation model on the NCCTG dataset and the control arms of the CA184-024 and CheckMate 066 trials (Figure 2B; black lines). Given the limited response rates of dacarbazine for metastatic melanoma (15%), the patients in the control arm were

280 regarded as untreated, and the model was fitted as such. For simplicity, we did not simulate dropout  
 281 or censoring in the trials shown in this paper, although it could be added to the simulation. On average,  
 282 the simulations capture the survival kinetics of the trials accurately, which is reflected by similar  
 283 median overall survival values and reasonably corresponding risk tables. The final step to fully  
 284 resemble late-stage immunotherapy trials in a simulation setting is replicating the treatment arms of  
 285 the CA184-024 and CheckMate 066 trials. These simulated patients were treated with ICI upon  
 286 diagnosis. ICI increased their T cell killing rate seven-fold and prolonged their survival, leading to OS  
 287 benefit in the *in silico* trial that matched the original trial. Hence, these *in silico* trials couple the disease  
 288 mechanism and mechanistic treatment effect to a realistic clinical trial outcome. Interestingly,  
 289 although not incorporated explicitly in our model, the trials show survival kinetics arising as a  
 290 consequence of the interaction between tumor and immune cells typically seen in immunotherapy  
 291 trials: a delayed curve separation and a plateau of the survival curve of the treatment arm at later  
 292 stages of the trial (Figure 2B (last two columns)).



293 **Figure 2: *In silico* cancer immunotherapy trials can generate a wide array of immunotherapy-specific survival kinetics.**

294 (A) Kaplan-Meier estimators of the NCCTG, CA184-024, and CheckMate 066 trials. While the NCCTG dataset is publicly  
 295 available<sup>30</sup>, the others are carefully reconstructed survival curves based on digitized data from their respective manuscripts  
 296 <sup>31, 32</sup>. (B) These trial simulations can mimic representative survival kinetics as observed in actual immunotherapy trials.  
 297 Specifically, typical immunotherapy-related survival kinetics – such as a delayed curve separation and a plateauing survival  
 298 curve in the treatment arm – arise from these simulations as emergent behavior. Note: We matched the risk table intervals  
 299 to the original manuscripts for comparative purposes.

300

301

302

***In silico* immunotherapy trials enable *a priori* prediction of trial outcomes and uncover**

303

**immunotherapy-specific response patterns**

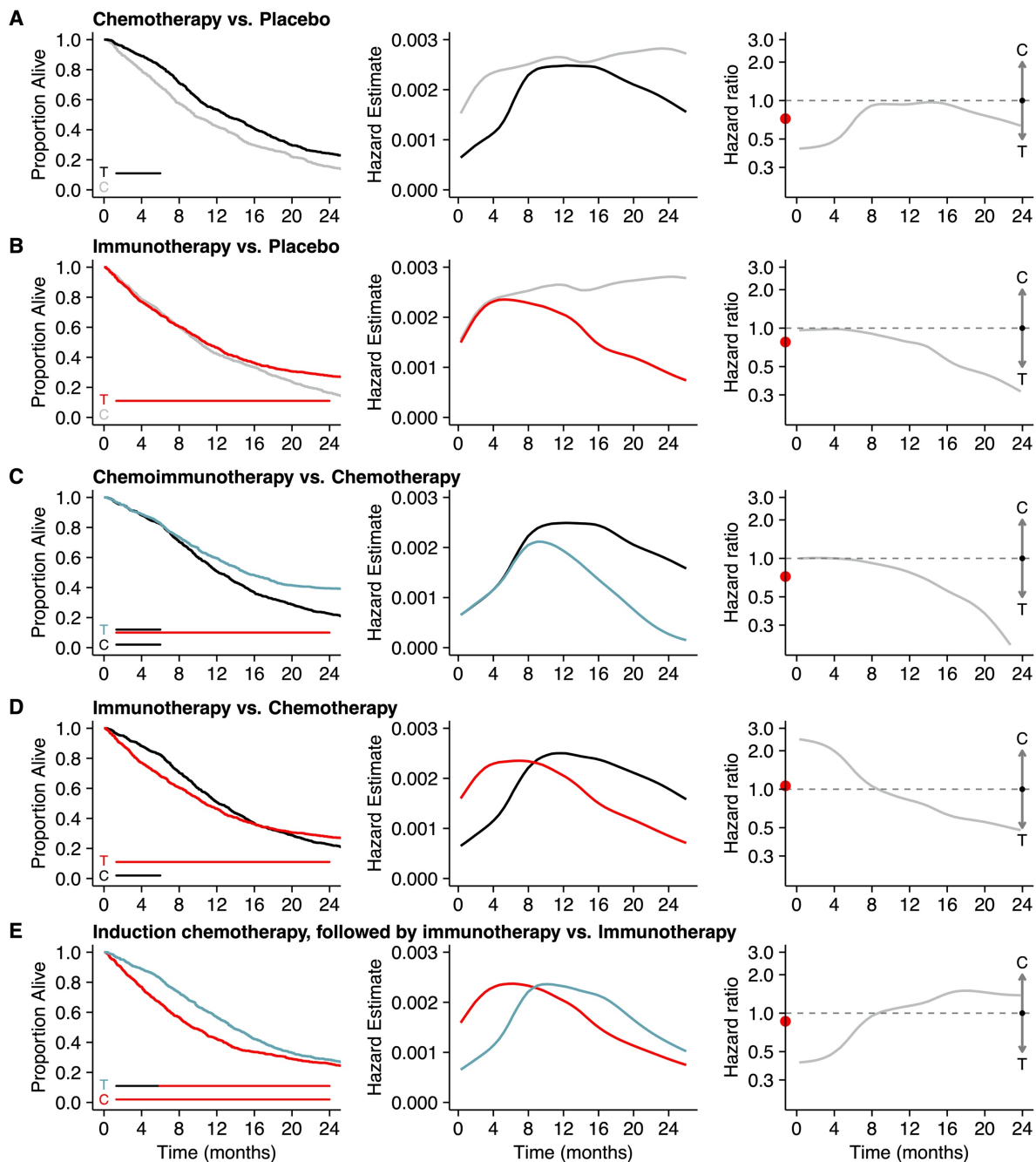
304

305 The design and the success rate of any clinical trial depends, among others, on an accurate *a priori*  
306 prediction of the survival kinetics – i.e., the shape of the survival curves and the trial outcome. For late-  
307 stage immunotherapy trials, commonly observed immunotherapy-induced response patterns are a  
308 delayed curve separation and a plateauing tail of the survival curve of the treatment arm (Figure 2).  
309 These characteristic survival curve shapes reveal a violation of a vital premise at the basis of many  
310 clinical trials: the proportional hazard assumption (PHA). The PHA states that the 'instantaneous death  
311 rate' of a patient (i.e., the hazard rate) in both arms of the trial should be proportional, resulting in a  
312 constant hazard ratio. Many traditional design methods, ranging from sample size calculations to  
313 outcome analyses, depend on this theory. For late-stage immunotherapy trials, this induces two  
314 problems: (1) while a violation of the PHA needs to be addressed during trial planning, the hazard rates  
315 – and thereby the fact if the trial adheres to or violates the PHA – become available *after* analysis of  
316 the trial, and (2) if a trial does not adhere to a PHA, what will be the shape of the survival kinetics?  
317 Especially in an era where treatment and control arm regimens are becoming increasingly complex,  
318 adjusting the design and analysis methods to unknown survival kinetics is challenging.

319 *In silico* clinical trials can provide principled estimates of the shape of the survival curve,  
320 including the underlying hazard rates and hazard ratios before trial execution. The most traditional  
321 scenario would be a trial in which patients are randomized 1:1 to mono-chemotherapy or placebo.  
322 Given the direct chemotherapy effect, the PHA is generally assumed to hold for these trials. An *in silico*  
323 trial in which chemotherapy reduces the tumor growth rate to 70% for the duration of the trial indeed  
324 replicates these assumptions (Supplementary Figure 2): the survival curves separate from the start of  
325 the trial, and the hazard ratio is constant over time. However, what happens if the chemotherapy  
326 effect does not last for the entire trial but for – maybe more realistically – 6 months? Initial  
327 proportional separation of the survival curves is followed by a nearly parallel decay of both curves,  
328 leading to an early survival benefit for the chemotherapy arm (Figure 3A). Consequently, for any  
329 therapy with a non-constant treatment effect – even for chemotherapy trials – deviations from the  
330 PHA might be observed. When we switch to immunotherapy in the treatment arm, a violated PHA  
331 becomes immediately apparent. Recall that in our model, immunotherapy exerts its mechanistic effect  
332 indirectly on the tumor via an increase in the killing rate of T cells. Through approximately the first six  
333 months, the hazard rates remain constant over time, but after that, they start to decline in the  
334 immunotherapy group (red line), yielding a non-constant hazard ratio over time (Figure 3B).

335 The flexibility of *in silico* trials lies in their ability to incorporate complex treatment regimens.  
336 For example, let us assume one would be interested in estimating the survival curves and underlying  
337 hazard ratio over time of a chemoimmunotherapy vs. chemotherapy trial (Figure 3C), an  
338 immunotherapy + chemotherapy-placebo vs. chemotherapy vs. immunotherapy-placebo trial (Figure  
339 3D), or a trial with induction chemotherapy followed by immunotherapy vs. immunotherapy (Figure

340 3E). Mechanism-based immunotherapy trials provide the means to translate biological assumptions  
 341 regarding the disease and treatment effects into survival kinetics (including its hazard rate/ratio  
 342 estimates). These survival kinetics, such as crossing survival curves (Figure 3D) or a temporary curve  
 343 separation (Figure 3E), may be hard to predict otherwise and can be detrimental for the trial outcome  
 344 if not dealt with appropriately.



345 **Figure 3: *In silico* clinical trials can predict immunotherapy-specific survival patterns based on biological assumptions.**  
 346 (A-E) Examples of 1:1 randomized trials with various (treatment) regimens (n=600 per arm). (A) A traditional chemotherapy  
 347 trial (vs. placebo) only shows a proportional hazard ratio when the biological treatment effect targets the tumor directly  
 348 and remains constant over time (compare to Supplementary Figure 2). (B) An *in silico* immunotherapy trial elicits typical  
 349 immunotherapy-induced survival kinetics (i.e., delayed curve separation) and violates the proportional hazard assumption.  
 350 (C-E) More intricate treatment or control regimens – (C) chemoimmunotherapy vs. chemotherapy, (D) immunotherapy +  
 351 chemotherapy-placebo vs. chemotherapy + immunotherapy-placebo, or (E) induction chemotherapy followed by  
 352 immunotherapy vs. immunotherapy – induce more complex survival kinetics, including (D) crossing survival curves or (E)  
 353 only a temporary separation of the survival curves. The horizontal bars in column 1 indicate the duration of the treatment effect  
 354

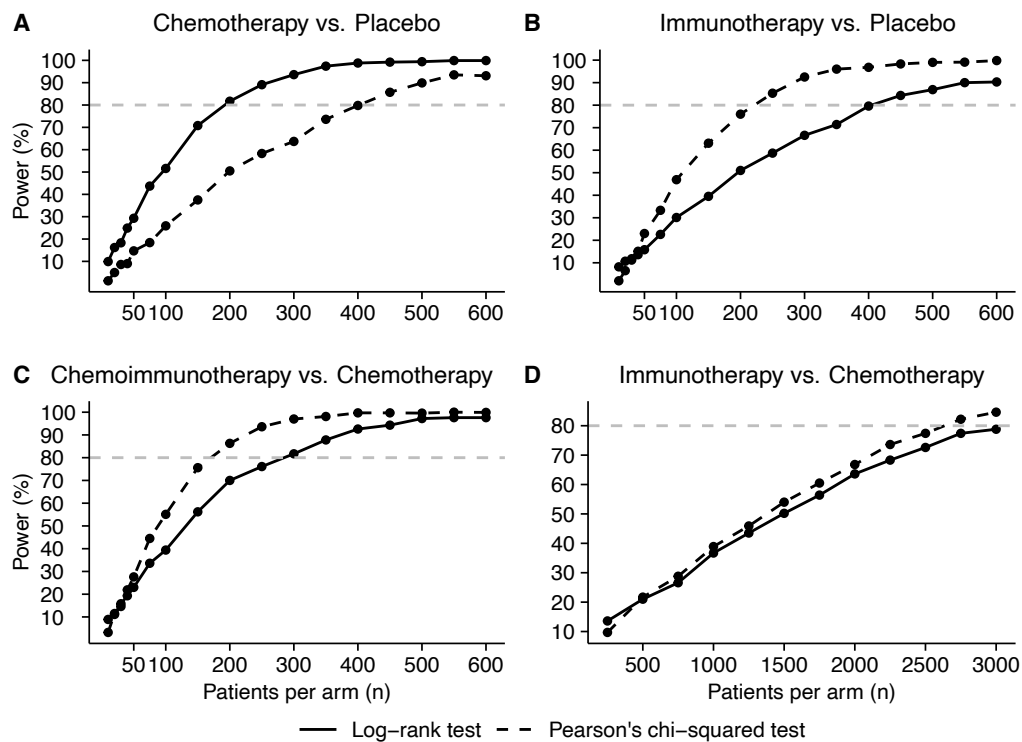
355 (T = treatment, C = control). The red dot in column three indicates the overall hazard ratio. For an accurate prediction of the  
356 hazard rates and hazard ratios, saturated survival curves (n=100.000 patients per arm) were used, and the data was smoothed  
357 before plotting.

358  
359 **Ignoring immunotherapy-specific response patterns might cause an overestimation of an**  
360 **immunotherapy trial's power**

361 To investigate the consequences of violating the PHA on the power of a clinical trial, we compared the  
362 power calculated using a PHA-dependent method (the Log Rank test) with a non-PHA-dependent  
363 method (Pearson's Chi-squared test) for different clinical scenarios. An essential difference between  
364 both methods is that the Log Rank test considers the entire survival curve, while Pearson's Chi-squared  
365 test only compares the number of events in both arms at 24 months. Logically, in a scenario that  
366 approximates the PHA the closest (such as a chemotherapy vs. placebo trial), a PHA-dependent  
367 method is superior (Figure 4A). However, a traditional immunotherapy trial violates the PHA, leading  
368 to a vast underestimation of the power of the trial when PHA-dependent methods are used for its  
369 planning (Figure 3B/4B). Given similar survival characteristics, this also holds for  
370 chemoimmunotherapy vs. chemotherapy trials (Figure 3C/4C). When survival curves cross during the  
371 trial, as seen in the immunotherapy vs. chemotherapy trial (Figure 3D), the PHA does not hold, and  
372 there is only a small survival benefit at 24 months for one of the arms of the trial. In this case, both  
373 methods predict the need for a large sample size to reach adequate power (Figure 4D). This insight  
374 indicates that it may be more rational to lengthen the trial's follow-up (i.e., a different endpoint)  
375 instead of increasing the number of participants; a finding that – on top of the absolute power –  
376 requires insight in the shape of the survival kinetics. As a general finding, ignoring immune-specific  
377 response patterns might induce an overestimation of a trial's current power, while in reality, a larger  
378 sample size (or a different endpoint) is necessary to establish the desired outcome.

379

380



381  
382 **Figure 4: A mismatch between survival kinetics and analysis methods induces an underestimation of the power of an**  
383 **immunotherapy trial.**

384 A power comparison using a PHA-dependent method (Log-rank test) or a PHA-independent method (Pearson's Chi-squared  
385 test) was made in different clinical scenarios: (A) a chemotherapy vs. placebo trial, (B) an immunotherapy vs. placebo trial,  
386 (C) a chemoimmunotherapy vs. chemotherapy trial, and (D) an immunotherapy vs. chemotherapy trial. Neglecting  
387 immunotherapy-specific response patterns while setting up a novel trial leads to a significant underestimation of the number  
388 of patients needed to show the efficacy of a treatment, thereby overestimating the power of the trial and reducing the  
389 probability of success.

390

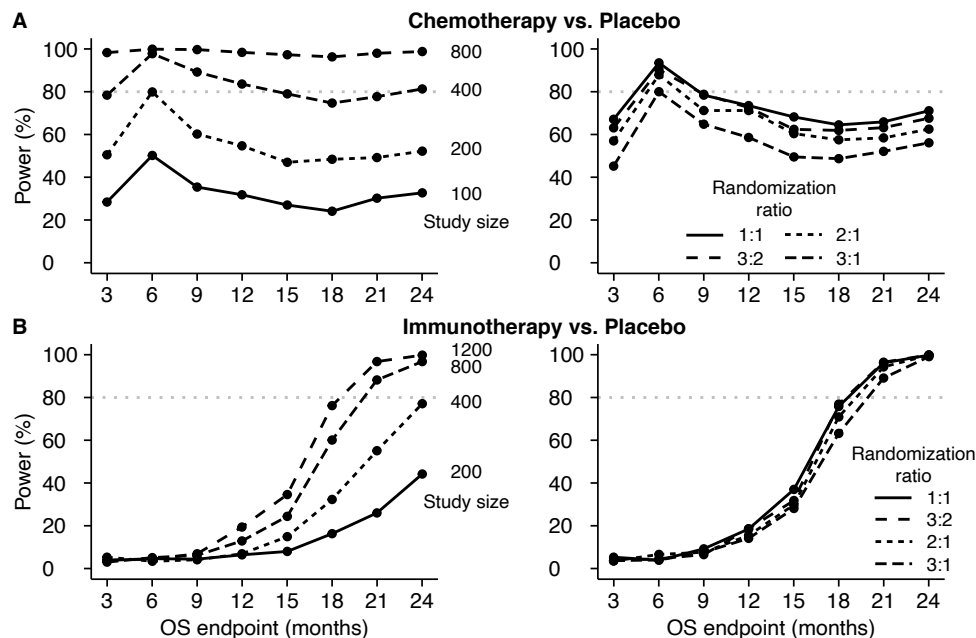
### 391 ***In silico* trials can validate endpoints and randomization ratios before trial execution**

392 Clearly, the success rate of novel immunotherapy trials depends on more than its sample size alone.

393 To establish an OS benefit of the treatment arm, it is crucial to analyze the trial once the data have  
394 reached a certain maturity – i.e., the treatment needs to be granted sufficient time to induce a survival  
395 benefit. We assumed that a delayed curve separation in immunotherapy trials would prolong the  
396 follow-up needed to establish an OS benefit of immunotherapy and thereby defer reaching maturity  
397 of the trial data. If the therapy is effective, data maturity can be regarded as the time point when a  
398 treatment effect can be observed. Hence, an optimal trial endpoint would be the earliest time at which  
399 this treatment effect can be detected with sufficient power. Therefore, we analyzed the power of  
400 differently sized trials with respect to their OS endpoint. Herein, we distinguished trials that were  
401 subject or were not subject to a delayed curve separation (immunotherapy and chemotherapy,  
402 respectively). In a classic chemotherapy trial, the treatment effect translates directly to a survival  
403 benefit in the treatment arm – the survival curves separate from the start. Therefore, the highest  
404 power will be obtained after the total duration of the treatment effect (Figure 5A, panel 1). In this case,  
405 the treatment effect lasts for six months, leading to the 6-months OS as the endpoint with the highest  
406 power. The delayed curve separation in immunotherapy trials renders it futile to analyze OS data early

407 on in the trial (Figure 5B, panel 1). A practical ramification is that in the presence of a delayed curve  
 408 separation, the trial requires a sufficiently long follow-up and an adequate size to gain power and  
 409 detect immunotherapy-specific treatment effects. Mechanism- and simulation-based power  
 410 calculations with *in silico* trials can consider these specific kinetics when determining the sample size  
 411 for upcoming trials.

412 Given the observation that both the size of an immunotherapy trial and its endpoint heavily  
 413 influence the probability of finding the survival benefit of interest, we presumed that increasing the  
 414 size of the treatment arm – i.e., an unequal randomization scheme – would similarly affect the power.  
 415 Instead of varying the study size, we now varied the randomization ratio (second panel of Figure 5A/B).  
 416 Interestingly, while the power logically depended on the OS endpoint, the randomization ratio did not  
 417 greatly affect the power (Figure 5B). Considering that an unequal treatment allocation may provide  
 418 ethical benefits, we confirm that the randomization ratio in immunotherapy trials is of secondary  
 419 importance compared to its size or primary OS endpoint. In summary, our *in silico* immunotherapy  
 420 trials replicate existing insights from trial design on how violation of the PHA affects power and analysis  
 421 choices. Our ability to directly translate biological assumptions on treatment mechanisms into survival  
 422 kinetics allows the researcher to reason in a principled manner about whether such violations of the  
 423 PHA would or would not be expected in their specific trial design and how the problem could be  
 424 addressed if it arises.



425 **Figure 5: *In silico* trials guide decisions on OS endpoints and randomization ratios of upcoming immunotherapy trials.**  
 426 **(A-B)** *In silico* trials can be used to find the optimal endpoint (panel 1) or randomization ratio (panel 2) of novel trials. **(A)**  
 427 Since the survival curves in classical chemotherapy trials separate from the trial onset, the highest power – and most optimal  
 428 endpoint – is obtained at the end of the treatment interval (i.e., after six months in this example; see Figure 3A). Although  
 429 less influential, a similar observation can be made for randomization ratios (study size panel 2: 300 patients). **(B)** Delayed  
 430 curve separation in immunotherapy trials emphasizes that a premature final analysis of the primary OS endpoint is  
 431 detrimental to the trial outcome. These trials permit validating the pre-specified survival outcomes of novel trials *a priori*.  
 432 Commonly selected randomization ratios do not seem to be heavily influenced by immunotherapy-specific response patterns  
 433 (study size panel 2: 1200 patient). Trial characteristics are similar to Figure 3A/B.

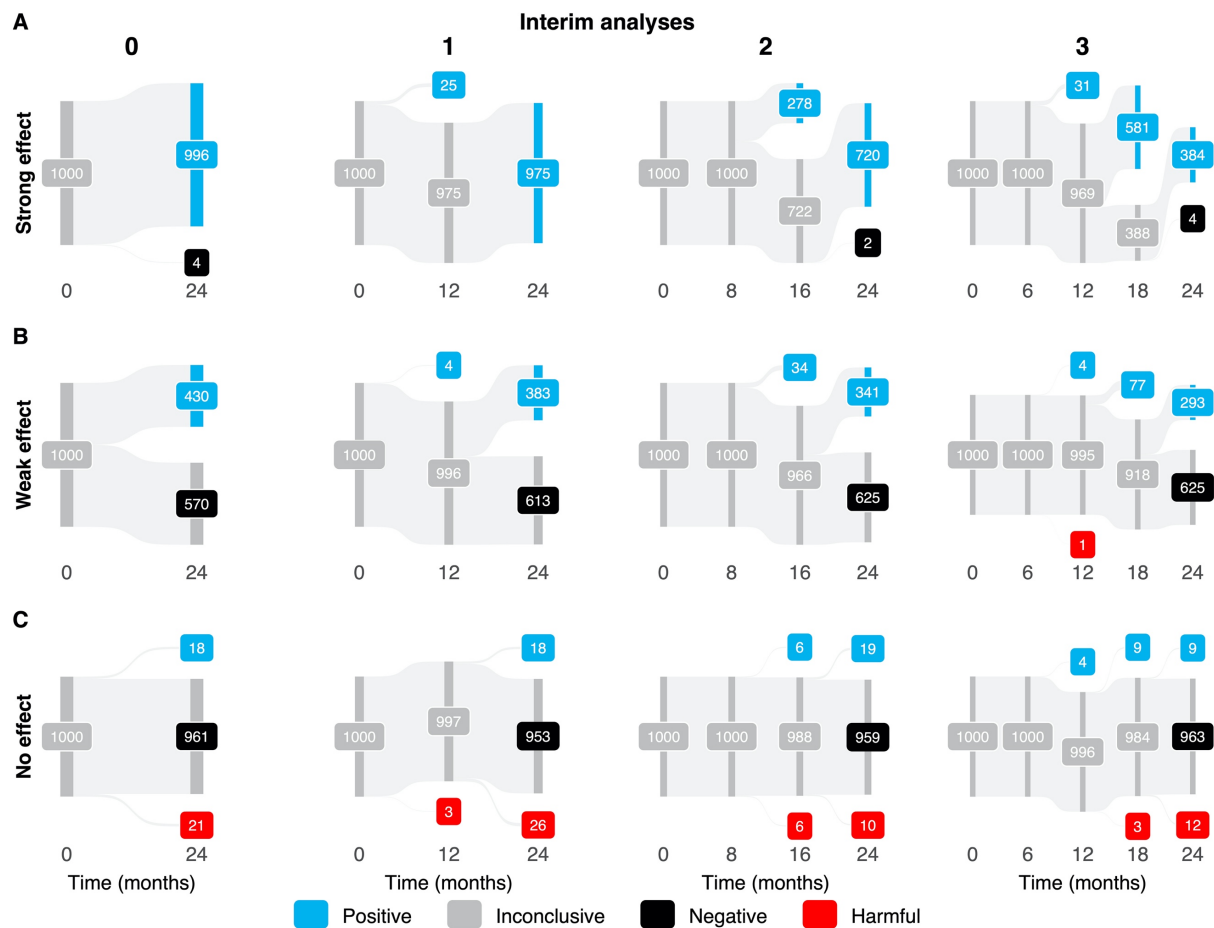
435

436 **Validating interim analyses to balance patient benefit and trial resources**

437 We have observed a clear tradeoff between the power of an immunotherapy trial on the one hand,  
438 and the primary OS endpoint, and correspondingly the data maturity, on the other. Luckily, the two  
439 are not entirely mutually exclusive: interim analyses have been developed for ethical purposes to  
440 establish positive or harmful treatment effects early. However, there is a catch: the necessity to control  
441 for multiple testing at each interim analysis lowers the significance threshold on the final analysis to  
442 maintain the same overall type I error rate. This begs the question: “How many interim analyses should  
443 you plan, and when should you plan them?” Again, principled answers to such questions can be  
444 obtained with the help of *in silico* immunotherapy trials. To illustrate this, we simulated 1000  
445 immunotherapy trials with 1200 patients per trial, randomized 1:1 over immunotherapy with a strong  
446 treatment effect or a placebo (Figure 6A). In the absence of interim analyses, the vast majority of the  
447 trials are predicted to end up positive. Adding interim analyses (O’Brien-Flemming approach) to the  
448 equation induces a tradeoff. On the one hand, increasing the number of equally-spaced interim  
449 analyses increases the probability of early detecting a positive treatment effect (e.g., approximately  
450 60% of the trials are positive after 18 months in the case of three interim analyses; Figure 6A). On the  
451 other hand, the overall probability of ending up with a negative trial due to more stringent analyses  
452 (i.e., less power) also increases, especially in the case of immunotherapies with a weaker treatment  
453 effect ( $\pm 57\%$  without an interim analysis vs.  $\pm 63\%$  with three interim analyses; Figure 6B). In an actual  
454 trial, the latter needs to be corrected by including additional patients to maintain the pre-planned  
455 power. Furthermore, we observe that the timing of the interim analysis is crucial. Whereas an interim  
456 analysis at 18 months provides additional value to the trial, interim analyses before 16 months are  
457 predicted to be wasteful: both due to the presence of non-proportional hazards and less mature data.  
458 As a control, we simulated trials without any treatment effect. By design, approximately 95% of the  
459 trials should end up negative irrespective of the number of interim analyses, which seemed to be the  
460 case (Figure 6C). Logically, the weaker the treatment effect, the higher the probability of erroneously  
461 finding a harmful treatment effect – a characteristic that the simulation also exhibits (Figure 6B/C).

462





463

464 **Figure 6: A priori validation of the interim analysis plan steers the selection of the optimal number and timing of the**  
 465 **analyses, avoids futile or even harmful analyses, and might optimize the use of trial resources.**

466 (A) In the case of immunotherapy with a potent effect, *in silico* trials help develop a rationale for the timing of the interim  
 467 analyses. While an interim analysis at 12 months might not add value to the trial, analyses after 16 and 18 months,  
 468 respectively, have a probability of approximately 28% and 60% to lead to early stopping with a positive result. (B) Multiple  
 469 interim analyses can reduce the probability of confirming the desired treatment effect in case of a weak immunotherapy  
 470 effect. (C) In the absence of any treatment effect (a control scenario), the number of interim analyses does not heavily  
 471 influence the trial outcome. Each trial simulation contains 1200 patients (randomization ratio 1:1) to ensure adequate power  
 472 of the trial. Trials are analyzed with a proportions test (Pearson's chi-squared test). Treatment effect (amplification factor of  
 473 T cell killing rate): strong = 7, weak = 3, no effect = 0 (see Methods).

474

## 475 DISCUSSION

476 In this study, we used mechanism-based *in silico* cancer immunotherapy trials to predict survival  
 477 kinetics and response profiles of novel immunotherapy trials. Complementary to conventional design  
 478 methods, *in silico* trials provide the ability to investigate the implications of a researcher's biological  
 479 (as opposed to statistical) hypotheses of a drug's mechanism of action for the design, conduct, analysis,  
 480 and outcome of clinical trials. When comparing the simulated outcomes to actual immunotherapy trial  
 481 outcomes, we showed that *in silico* trials are suited to translate complex biological mechanisms (such  
 482 as observed during the treatment of patients with ICI) into realistic trial outcomes. Crucially, the  
 483 survival kinetics that arose from these mechanism-based simulations reflected two pivotal  
 484 components often found in immunotherapy trials: a delayed curve separation and a plateauing tail of

485 the survival curve at later stages of the trial. In line with genuine immunotherapy trials, we find that  
486 these immunotherapy-specific response patterns differ considerably from chemotherapy-based  
487 kinetics. Our findings confirm that diversity in survival kinetics profoundly impacts the outcomes of  
488 immunotherapy trials<sup>33</sup>. Consequently, these features need to be considered when deciding on the  
489 sample size, endpoint, randomization ratio, and the number and timing of interim analyses of a novel  
490 immunotherapy trial.

491 Over the past two decades, *in silico* clinical trials are gaining in popularity. These trials enable  
492 investigating, among others, how novel drugs, treatment schedules, dosing regimens, and interpatient  
493 heterogeneity affect the outcome of a clinical trial<sup>34</sup>. *In silico* clinical studies have a wide range of  
494 applicability from pediatric infectious<sup>35</sup> and orphan diseases<sup>36</sup> to diabetes<sup>37</sup>, inflammatory  
495 autoimmune diseases<sup>38</sup>, traumatic injury<sup>39</sup>, psychiatric illness<sup>40</sup>, and cancer. In oncology, several *in*  
496 *silico* clinical trials involving chemotherapy and tyrosine kinase inhibitors have been performed<sup>41, 42</sup>.  
497 Moreover, with the onset of checkpoint inhibitors, *in silico* immunotherapy trials have gained interest,  
498 leading to trials with anti-CTLA-4-antibodies and anti-PD-(L)1 antibodies<sup>43, 44, 45</sup>. The common  
499 denominator in these trials is that they primarily center around the therapies' dosing regimens and  
500 treatment schedules. Herein lies the main difference with our simulation approach: although the 'key  
501 ingredients' of these approaches are similar – they are based on a mathematical abstraction of a  
502 disease mechanism – our trials do not aim to optimize treatment schedules. Instead, we complement  
503 traditional design methodology by adding the means to predict trial outcomes and elucidate trial  
504 kinetics *a priori* to steer design decisions of novel immunotherapy trials. These trials differ from  
505 traditional trial design research in that these, often statistically-grounded, approaches simulate clinical  
506 trials based on population-level assumptions (e.g., with particular distributions of survival times, study  
507 durations, or with a specific censoring mechanism). Examples of these high-level simulation  
508 approaches include, but are certainly not limited to, studies aiming to calculate the sample size and  
509 power of clinical trials<sup>46,47,48</sup>. Since these methods lack a direct link to the underlying biological disease  
510 mechanism, interpreting their parameters for individual trial participants is difficult or even  
511 impossible. In contrast, *in silico* trials are founded on biological assumptions but then translate these  
512 assumptions into statistical concepts such as hazard ratio kinetics. In this manner, simulated trials  
513 encourage an interdisciplinary discussion about the design of an upcoming trial.

514 *In silico* clinical trials are applicable in several settings. First, they provide the means to verify  
515 clinical trial and treatment assumptions before investing extensive amounts of work and funds into  
516 the development and execution of a clinical trial and can, thereby, function as a proof of principle of  
517 the soundness of the hypotheses for an upcoming trial. Scrutinizing each aspect of the trial supports  
518 optimal design decisions and might reduce unanticipated outcomes. Moreover, this mechanism-based  
519 approach does not necessitate a deep understanding of complex mathematical theorems; instead, it

520 requires a biological understanding of a disease. This mechanistic basis is intuitive, which benefits the  
521 communication between clinical doctors and biomedical researchers on the one hand and statisticians  
522 and clinical trialists on the other. Additionally, *in silico* trials might serve as excellent educational tools.  
523 The ability to simulate a wide range – from basic to highly advanced – research questions can be  
524 exploited in teaching activities for entry-level clinicians to experienced trialists. A final implication,  
525 which holds for any trial simulation, is that they may provide insight when conventional clinical trials  
526 are unfeasible due to practical or ethical constraints (e.g., clinical trials in rare diseases, pediatrics, or  
527 critical care medicine).

528         Nonetheless, *in silico* clinical trials have to be considered in light of some limitations. The most  
529 critical limitation is universal to *any* – either *in vitro*, *in vivo*, or computational – scientific model: the  
530 immunotherapy trial outcomes depend heavily (if not entirely) on the biological assumptions of the  
531 model, meaning that incorrect interactions or erroneous parametrization of the model might induce  
532 inaccurate outcomes. The parameterization, in particular, might pose a problem: given the often novel  
533 treatment mechanisms, data to fine-tune the parameters of the model accurately might be scarce. In  
534 these cases, the simulation itself can be used as a sensitivity analysis to assess to what extent a certain  
535 parameter range influences the robustness of the predictions. In addition, while the model itself is  
536 intuitive to understand, translating biological principles into an ODE model and implementing it into a  
537 simulation requires thorough knowledge of computational methods, limiting its widespread  
538 applicability.

539         In summary, *in silico* cancer immunotherapy trials offer a versatile approach to simulate  
540 immunotherapy trials based on biological assumptions. Furthermore, as a simulation tool, they  
541 facilitate the verification of trial design decisions to optimize the probability of a successful  
542 immunotherapy trial and contribute to high-quality research for cancer patients.

543  
544

545 **REFERENCES**

- 546 1. Upadhaya S, Hubbard-Lucey VM, Yu JX. Immuno-oncology drug development forges on despite  
547 COVID-19. *Nat Rev Drug Discov*, (2020).  
548
- 549 2. Dowden H, Munro J. Trends in clinical success rates and therapeutic focus. *Nat Rev Drug Discov*  
550 **18**, 495-496 (2019).  
551
- 552 3. Wong CH, Siah KW, Lo AW. Estimation of clinical trial success rates and related parameters.  
553 *Biostatistics* **20**, 273-286 (2019).  
554
- 555 4. Thomas D, *et al.* Clinical Development Success Rates and Contributing Factors 2011-2020.).  
556 BIO, Informa Pharma Intelligence, QLS Advisors (2021).  
557
- 558 5. Hwang TJ, Carpenter D, Lauffenburger JC, Wang B, Franklin JM, Kesselheim AS. Failure of  
559 Investigational Drugs in Late-Stage Clinical Development and Publication of Trial Results. *JAMA*  
560 *Intern Med* **176**, 1826-1833 (2016).  
561
- 562 6. de Miguel M, Calvo E. Clinical Challenges of Immune Checkpoint Inhibitors. *Cancer Cell* **38**, 326-  
563 333 (2020).  
564
- 565 7. Li A, Bergan RC. Clinical trial design: Past, present, and future in the context of big data and  
566 precision medicine. *Cancer* **126**, 4838-4846 (2020).  
567
- 568 8. Cousin S, Seneschal J, Italiano A. Toxicity profiles of immunotherapy. *Pharmacol Ther* **181**, 91-  
569 100 (2018).  
570
- 571 9. Seymour L, *et al.* iRECIST: guidelines for response criteria for use in trials testing  
572 immunotherapeutics. *Lancet Oncol* **18**, e143-e152 (2017).  
573
- 574 10. Hoos A, *et al.* Improved endpoints for cancer immunotherapy trials. *J Natl Cancer Inst* **102**,  
575 1388-1397 (2010).  
576
- 577 11. Chen TT. Statistical issues and challenges in immuno-oncology. *J Immunother Cancer* **1**, 18  
578 (2013).  
579
- 580 12. Mick R, Chen TT. Statistical Challenges in the Design of Late-Stage Cancer Immunotherapy  
581 Studies. *Cancer Immunol Res* **3**, 1292-1298 (2015).  
582
- 583 13. Rahman R, *et al.* Deviation from the Proportional Hazards Assumption in Randomized Phase 3  
584 Clinical Trials in Oncology: Prevalence, Associated Factors, and Implications. *Clin Cancer Res*  
585 **25**, 6339-6345 (2019).  
586
- 587 14. Hodi FS, *et al.* Immune-Modified Response Evaluation Criteria In Solid Tumors (imRECIST):  
588 Refining Guidelines to Assess the Clinical Benefit of Cancer Immunotherapy. *J Clin Oncol* **36**,  
589 850-858 (2018).  
590
- 591 15. Wolchok JD, *et al.* Guidelines for the evaluation of immune therapy activity in solid tumors:  
592 immune-related response criteria. *Clin Cancer Res* **15**, 7412-7420 (2009).  
593
- 594 16. Anagnostou V, *et al.* Immuno-oncology Trial Endpoints: Capturing Clinically Meaningful  
595 Activity. *Clin Cancer Res* **23**, 4959-4969 (2017).  
596

- 597 17. Mushti SL, Mulkey F, Sridhara R. Evaluation of Overall Response Rate and Progression-Free  
598 Survival as Potential Surrogate Endpoints for Overall Survival in Immunotherapy Trials. *Clin*  
599 *Cancer Res* **24**, 2268-2275 (2018).  
600
- 601 18. Chen TT. Milestone Survival: A Potential Intermediate Endpoint for Immune Checkpoint  
602 Inhibitors. *J Natl Cancer Inst* **107**, (2015).  
603
- 604 19. Kaufman HL, *et al.* Durable response rate as an endpoint in cancer immunotherapy: insights  
605 from oncolytic virus clinical trials. *J Immunother Cancer* **5**, 72 (2017).  
606
- 607 20. Chan TA, *et al.* Development of tumor mutation burden as an immunotherapy biomarker:  
608 utility for the oncology clinic. *Ann Oncol* **30**, 44-56 (2019).  
609
- 610 21. Dudley JC, Lin MT, Le DT, Eshleman JR. Microsatellite Instability as a Biomarker for PD-1  
611 Blockade. *Clin Cancer Res* **22**, 813-820 (2016).  
612
- 613 22. Patel SP, Kurzrock R. PD-L1 Expression as a Predictive Biomarker in Cancer Immunotherapy.  
614 *Mol Cancer Ther* **14**, 847-856 (2015).  
615
- 616 23. Sha D, Jin ZH, Budczies J, Kluck K, Stenzinger A, Sinicrope FA. Tumor Mutational Burden as a  
617 Predictive Biomarker in Solid Tumors. *Cancer Discovery* **10**, 1808-1825 (2020).  
618
- 619 24. Chen TT. Designing Late-Stage Randomized Clinical Trials with Cancer Immunotherapy: Can  
620 We Make It Simpler? *Cancer Immunol Res* **6**, 250-254 (2018).  
621
- 622 25. Royston P, Parmar MK. Restricted mean survival time: an alternative to the hazard ratio for  
623 the design and analysis of randomized trials with a time-to-event outcome. *BMC Med Res*  
624 *Methodol* **13**, 152 (2013).  
625
- 626 26. Xu Z, Zhen B, Park Y, Zhu B. Designing therapeutic cancer vaccine trials with delayed treatment  
627 effect. *Stat Med* **36**, 592-605 (2017).  
628
- 629 27. Creemers JHA, *et al.* A tipping point in cancer-immune dynamics leads to divergent  
630 immunotherapy responses and hampers biomarker discovery. *J Immunother Cancer* **9**, (2021).  
631
- 632 28. Borghans JA, de Boer RJ, Segel LA. Extending the quasi-steady state approximation by changing  
633 variables. *Bull Math Biol* **58**, 43-63 (1996).  
634
- 635 29. Gadhamsetty S, Maree AF, Beltman JB, de Boer RJ. A general functional response of cytotoxic  
636 T lymphocyte-mediated killing of target cells. *Biophys J* **106**, 1780-1791 (2014).  
637
- 638 30. Loprinzi CL, *et al.* Prospective evaluation of prognostic variables from patient-completed  
639 questionnaires. North Central Cancer Treatment Group. *J Clin Oncol* **12**, 601-607 (1994).  
640
- 641 31. Maio M, *et al.* Five-year survival rates for treatment-naïve patients with advanced melanoma  
642 who received ipilimumab plus dacarbazine in a phase III trial. *J Clin Oncol* **33**, 1191-1196 (2015).  
643
- 644 32. Ascierto PA, *et al.* Survival Outcomes in Patients With Previously Untreated BRAF Wild-Type  
645 Advanced Melanoma Treated With Nivolumab Therapy: Three-Year Follow-up of a  
646 Randomized Phase 3 Trial. *JAMA Oncol* **5**, 187-194 (2019).  
647

- 648 33. Chen TT. Predicting analysis times in randomized clinical trials with cancer immunotherapy.  
649 *BMC Med Res Methodol* **16**, 12 (2016).  
650
- 651 34. Alfonso S, Jenner AL, Craig M. Translational approaches to treating dynamical diseases through  
652 in silico clinical trials. *Chaos* **30**, 123128 (2020).  
653
- 654 35. Valitalo PA, *et al.* Novel model-based dosing guidelines for gentamicin and tobramycin in  
655 preterm and term neonates. *J Antimicrob Chemother* **70**, 2074-2077 (2015).  
656
- 657 36. Carlier A, Vasilevich A, Marechal M, de Boer J, Geris L. In silico clinical trials for pediatric orphan  
658 diseases. *Sci Rep* **8**, 2465 (2018).  
659
- 660 37. Klinke DJ, 2nd. Integrating epidemiological data into a mechanistic model of type 2 diabetes:  
661 validating the prevalence of virtual patients. *Ann Biomed Eng* **36**, 321-334 (2008).  
662
- 663 38. Schmidt BJ, Casey FP, Paterson T, Chan JR. Alternate virtual populations elucidate the type I  
664 interferon signature predictive of the response to rituximab in rheumatoid arthritis. *BMC*  
665 *Bioinformatics* **14**, 221 (2013).  
666
- 667 39. Brown D, *et al.* Trauma in silico: Individual-specific mathematical models and virtual clinical  
668 populations. *Sci Transl Med* **7**, 285ra261 (2015).  
669
- 670 40. Magnusson MO, *et al.* Dosing and Switching Strategies for Paliperidone Palmitate 3-Month  
671 Formulation in Patients with Schizophrenia Based on Population Pharmacokinetic Modeling  
672 and Simulation, and Clinical Trial Data. *CNS Drugs* **31**, 273-288 (2017).  
673
- 674 41. Perez-Garcia VM, *et al.* Computational design of improved standardized chemotherapy  
675 protocols for grade II oligodendrogliomas. *PLoS Comput Biol* **15**, e1006778 (2019).  
676
- 677 42. Fassoni AC, Baldow C, Roeder I, Glauche I. Reduced tyrosine kinase inhibitor dose is predicted  
678 to be as effective as standard dose in chronic myeloid leukemia: a simulation study based on  
679 phase III trial data. *Haematologica* **103**, 1825-1834 (2018).  
680
- 681 43. Jafarnejad M, *et al.* A Computational Model of Neoadjuvant PD-1 Inhibition in Non-Small Cell  
682 Lung Cancer. *AAPS J* **21**, 79 (2019).  
683
- 684 44. Milberg O, *et al.* A QSP Model for Predicting Clinical Responses to Monotherapy, Combination  
685 and Sequential Therapy Following CTLA-4, PD-1, and PD-L1 Checkpoint Blockade. *Sci Rep* **9**,  
686 11286 (2019).  
687
- 688 45. Wang H, *et al.* In silico simulation of a clinical trial with anti-CTLA-4 and anti-PD-L1  
689 immunotherapies in metastatic breast cancer using a systems pharmacology model. *R Soc*  
690 *Open Sci* **6**, 190366 (2019).  
691
- 692 46. Bang H, Jung SH, George SL. Sample size calculation for simulation-based multiple-testing  
693 procedures. *J Biopharm Stat* **15**, 957-967 (2005).  
694
- 695 47. Doostfatemeh M, Taghi Ayatollah SM, Jafari P. Power and Sample Size Calculations in Clinical  
696 Trials with Patient-Reported Outcomes under Equal and Unequal Group Sizes Based on Graded  
697 Response Model: A Simulation Study. *Value Health* **19**, 639-647 (2016).  
698

699 48. Wilson DT, Hooper R, Brown J, Farrin AJ, Walwyn RE. Efficient and flexible simulation-based  
700 sample size determination for clinical trials with multiple design parameters. *Stat Methods*  
701 *Med Res* **30**, 799-815 (2021).

702  
703

#### 704 **LIST OF ABBREVIATIONS**

705 ICI: immune checkpoint inhibitor; NCCTG: North Central Cancer Treatment Group; ODE: ordinary  
706 differential equation; OS: overall survival; PHA: proportional hazard assumption.

707

#### 708 **DECLARATIONS**

##### 709 **Ethics approval and consent to participate**

710 Not applicable.

711

##### 712 **Consent for publication**

713 Not applicable.

714

##### 715 **Availability of data and material**

716 The code is available at GitHub: <https://github.com/jeroencreemers/in-silico-clinical-trials>

717

##### 718 **Competing interests**

719 Not applicable

720

##### 721 **Funding**

722 JC was funded by the Radboudumc. CF received an ERC Adv Grant ARTimmune (834618) and an NWO  
723 Spinoza grant. IV received an NWO-Vici grant (918.14.655). JT was supported by a Young Investigator  
724 Grant (10620) from the Dutch Cancer Society and an NWO grant (VI.Vidi.192.084).

725

##### 726 **Authors' contribution**

727 JHAC and JT conceived this study. JHAC performed the experiments and wrote the manuscript under  
728 the supervision of JT. All authors provided feedback on the manuscript and reviewed the manuscript  
729 prior to submission.

730

##### 731 **Acknowledgments**

732 Not applicable.

733